ON STRUCTURAL INTEGRITY ASSESSMENT OF POWER TRANSFORMERS UNDER DYNAMIC TRANSPORTATION LOADS

Fernando Torres Pereira da Silva
Larissa Driemeier
University of São Paulo - Polytechnic School
ftorresps@usp.br
driemeie@usp.br

Abstract. Power transformers, as non serialized products, are subject to a number of process deviations. The divergences that transformers present from their original design may have consequences on their ability to withstand mechanical loads which will be applied on them. Their transportation from workshop to power plants is one of the main events their structures are loaded. This work focuses on describing and analyzing a generic power transformer in a two-dimensional model, under the sight of Analytical Mechanics and Structural Reliability in order to identify important parameters related to their structural integrity, especially those concerning the failure mode of dismantling of the ferromagnetic core in the step-lap joints. The numerical model of the transformer consists of a representation of rigid bodies, connected to each other by stiffness and damping elements, having the assembly of the ferromagnetic core more detailed in order to describe the friction present on their step-lap joint. The evaluation of friction in these locations is made using the Lagrange Multipliers Method, by considering it as a movement restriction, and the limit values of forces and moments to which the planar sliding of the core sheets occurs, damaging the behavior of the electric machine, are determined using Newton-Raphson and Optimization Methods.

Keywords: Power Transformers, Transportation, Structural Reliability, Lagrangian Mechanics, Numerical Methods

1. INTRODUCTION

A power transformer is one of the most important accouterments of national electric grid. Once its working life varies from twenty to thirty years, it's absolutely necessary that the equipment be fully functional at its supply, taking account of the growth of power demand during its life cycle.

Before commissioning the equipment, however, the transformer is subjected to random mechanical loads resulting from its transportation. The ability of power transformers to withstand these loads is strongly dependent on the manufacturing process. The accomplishment of the design requirements must be ensured in the whole manufacture. Nevertheless, as a consequence of the factory flexibility to different sizes and types of equipment, deviations that might affect its integrity are, sometimes, introduced in the product.

Not only is the manufacture process a source of deviations from the original design, the dynamic response of transportation vehicles, the unevenness of lanes and urgent situations during its course are unknown at the design phase. Despite these situations, the transformer shall remain reliable when finally in operation. These facts motivated the investigations explored in this article.

In order to assess the operational condition of power transformers in the moment they arrive their final destination, a number of techniques have been employed in the late years and studies have been performed in order to identify more precisely the significance of those results.

In Sim *et al.* (2004) some techniques are presented, not restricting to those related to the assessment of transformers after transportation. They are classified in two basic categories: assessment of transformer in and out of operation. The in-operation assessment techniques have the objective of identifying failures in electric insulation, either by analyzing dissolved gases in oil or by identifying partial discharges. The out-of-operation assessment techniques are employed when there is a risk in energizing the equipment, after of transportation, for instance. Internal movements and loss of electric insulation are the main parameters to be identified with them.

In Secue and Mombello (2008) is presented one of the non-invasive assessment methods of the transformer condition when out of operation, named Sweep Frequency Response Analysis (*SFRA*). This method is a non-intrusive test that can be carried out for any voltage rating of power transformer, generator transformer and distribution transformer. It injects sinusoidal low voltage signals of varying frequencies into one side of the winding and measures the output signals in order to obtain the winding transfer function. Its employment on detecting internal movements or windings deformation is described in the article, explaining that the changes of the capacitive effects of the equipment are associated with the these movements.

In Pleite *et al.* (2006) is described the use of the same technique to detect failures in the ferromagnetic core. It is mentioned the difficulty of the technique use in order to detect specific failures of the transformer, once it provides a landscape of the equipment condition as a whole. Methods for specific identification of core failures are, then, presented.

Given that the Sweep Frequency Response Analysis is a comparative method, an initial signature of the transformer's condition is necessary to evaluate any possible damage. In Pleite *et al.* (2002) is presented a transformer's modeling in terms of associated resistances, inductances and capacitances in order to estimate results based on the design values.

Dick and Erven (1978) presents the results obtained from the first implementation of *SFRA* in power transformers in Industry. Its advantages over the Low Voltage Impulse technique (*LVI*), which is method of detecting transformer winding movement based on taking a signature of it via a short low voltage impulse (300 V) applied in one winding and recording the capacitively coupled current in another winding, are presented.

As demonstrated previously, the health of power transformers after arriving the electrical substation is a major concern for Industry, which has been searching ways for mitigating critical damages.

Therefore, this study proposes itself analyzing the transmission of mechanical loads from vehicles to the equipment, focusing on its influence on the emerging of failures.

Consequently, it is investigated, also, the sensitivity of the mechanical system to design deviations or load variations.

The main parts of the equipment here studied that are transported together are the tank, the set of ferromagnetic core and windings, also called *active part* and its internal electric connections. The types of damage which can affect power transformers are diverse: from simple external painting damage on the tank to relative movement of the active part inside the tank (which decreases electrical distances) due to breaking of its arresting devices or even movements of magnetic core steel sheets (which imply loss of efficiency or unbalance of magnetic flux) which, despite being mechanically restrained from moving, are mainly kept in place by the friction among them.

2. MODELING OF THE MECHANICAL SYSTEM

In order to accomplish the proposed objective, it was modeled the mechanical system of a generic power transformer in the longitudinal plane according to the transportation direction. The mechanical system is divided into five rigid bodies connected by spring-damper elements.

The rigid bodies of the mechanical system, in accordance with Fig. 1, are:

1. The active part of the transformer, excluding the two most extreme core limbs;

2. The frontal core limb (according the transportation direction);

3. The back core limb;

4. The upper part of the transformer's tank;

5. The lower part of the transformer's tank and the transportation vehicle
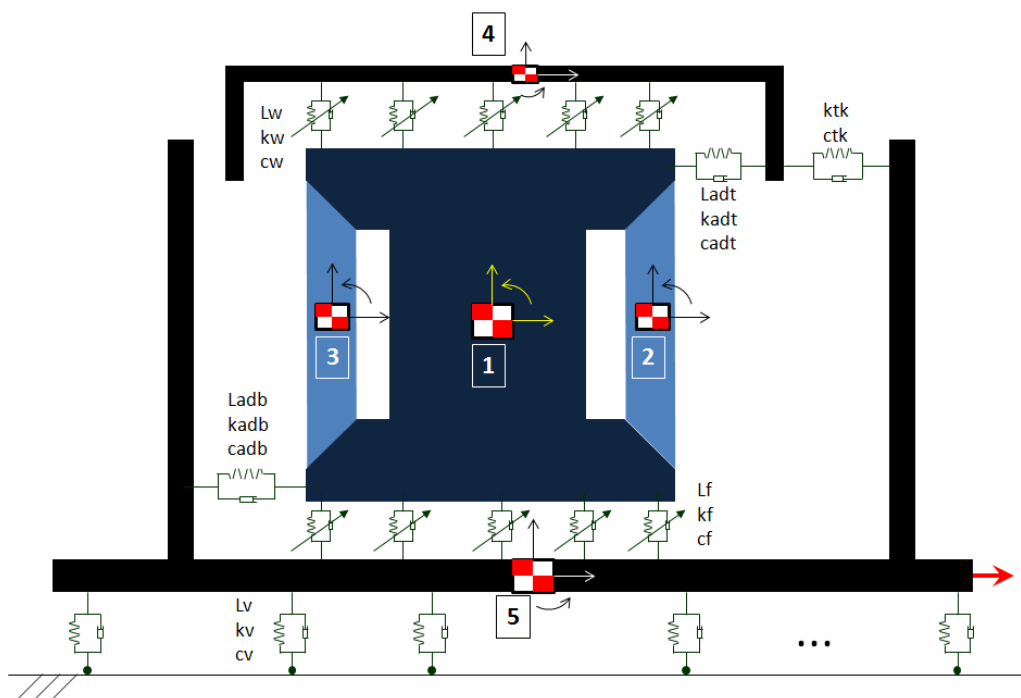
Figure 1: Mechanical Model of a Power Transformer being Transported

The spring-damper elements presented in the mechanical system are simplifications of the following connections among bodies:

- *Vehicle Suspension System*: represented by the set of properties L_v, k_v and c_v;

- *Active Part's Top Arresting Devices*: represented by the set of properties L_{adt}, k_{adt} and c_{adt};

- *Active Part's Bottom Arresting Devices*: represented by the set of properties L_{adb}, k_{adb} and c_{adb};

- *Active Part's Feet Plates*: represented by the set of properties L_f, k_f and c_f;

- *Active Part's Top Wooden Blocks*: represented by the set of properties L_w, k_w and c_w;

- *Tank Flexibility*: represented by the properties k_{tk} and c_{tk};

The top and bottom arresting devices are represented in a simplified manner in Fig. 1 as just single elements. In fact, they can be several of them along the active part. The representation was done this way in order not to make the figure polluted.

The mathematical modeling of the mechanical system was performed adopting the analytical Lagrangian formalism. The parameters that were chosen as the generalized coordinates (**q**) are:

- $x_1 \cdots x_5$: horizontal coordinates of the rigid bodies;

- $y_1 \cdots y_5$: vertical coordinates of the rigid bodies;

- $\theta_1 \cdots \theta_5$: rotation angle of the rigid bodies according to the horizontal axis transversal to the transportation direction (*Pitch angles*);

Hence, it was performed the evaluation of kinetic and potential energy.

$$T = \sum_{i=1}^{5} \frac{m_i \left(\dot{x}_i^2 + \dot{y}_i^2 \right)}{2} + \frac{J_i \dot{\theta}_i^2}{2} \tag{1}$$

$$
\begin{aligned}
U &= U_g + U_v + U_{adt} + U_{adb} + U_f + U_w + U_{tk} \\
&= \sum_{i=1}^{5} m_i y_i g + \sum_{j=1}^{N_v} \frac{k_{v_j} \delta_{v_j}^2}{2} + \sum_{k=1}^{N_{adt}} \frac{k_{adt_k} \delta_{adt_k}^2}{2} + \sum_{n=1}^{N_{adb}} \frac{k_{adb_n} \delta_{adb_n}^2}{2} + \sum_{p=1}^{N_f} \frac{k_{f_p} \delta_{f_p}^2}{2} \mathrm{H}(-\delta_{f_p}) + \\
&\quad + \sum_{r=1}^{N_w} \frac{k_{w_r} \delta_{w_r}^2}{2} \mathrm{H}(-\delta_{w_r}) + \frac{k_{tk} \delta_{tk}^2}{2}
\end{aligned}
\tag{2}
$$

where:

- U_g is the gravitational potential energy;

- U_v, U_{adt}, U_{adb}, U_f, U_w, U_{tk} are the elastic potential energy of the spring-damper elements;

- m_i is the mass of the ith rigid body of the system;

- J_i is the moment of inertia in relation to the horizontal axis transversal to transportation direction (*pitch axis*) of the ith rigid body of the system;

- $(\dot{\ })$ represents the first order time-derivative of a parameter of the mechanical system;

- $\mathrm{H}(\cdot)$ is the Heaviside distribution;

- N_v, N_{adt}, N_{adb}, N_f and N_w are the total amount of each spring-damper element considered in the mechanical system;

- δ_v, δ_{adt}, δ_{adb}, δ_f, δ_w, δ_{tk} are the elongations of the spring-damper elements, evaluated in terms of the generalized coordinates.

The elements of the active part's feet plates and top wooden blocks, represented in Fig. 1 by variable spring-damper elements, in fact, represent contact connections. So, in order to describe this behavior, the potential energy of these elements are only computed when in compression. Therefore, the Heaviside distribution was included in the formulation to impose that only when the elongation is negative (compression) these terms are taken into account.

The Lagrangian function, $\mathcal{L}$, of the mechanical system is given by:

$$\mathcal{L} = T - U \tag{3}$$

The damping in the mechanical system is computed by the evaluation the *Rayleighian Dissipation Function*, $\mathcal{F}$, in the spring-damper elements.

$$
\begin{aligned}
\mathcal{F} \quad = \quad & \mathcal{F}_v + \mathcal{F}_{adt} + \mathcal{F}_{adb} + \mathcal{F}_f + \mathcal{F}_w + \mathcal{F}_{tk} \\
= \quad & \sum_{j=1}^{N_v} \frac{c_{v_j} \dot{\delta}_{v_j}^2}{2} + \sum_{k=1}^{N_{adt}} \frac{c_{adt_k} \dot{\delta}_{adt_k}^2}{2} + \sum_{n=1}^{N_{adb}} \frac{c_{adb_n} \dot{\delta}_{adb_n}^2}{2} + \sum_{p=1}^{N_f} \frac{c_{f_p} \dot{\delta}_{f_p}^2}{2} \mathrm{H}(-\delta_{f_p}) + \\
& + \sum_{r=1}^{N_w} \frac{c_{w_r} \dot{\delta}_{w_r}^2}{2} \mathrm{H}(-\delta_{w_r}) + \frac{c_{tk} \dot{\delta}_{tk}^2}{2}
\end{aligned} \tag{4}
$$

At this moment, it is necessary to define the *Nabla Operators* in terms of the generalized coordinates and velocities:

$$\nabla^q = \left\{ \frac{\partial}{\partial x_1}, \cdots, \frac{\partial}{\partial x_5}, \frac{\partial}{\partial y_1}, \cdots, \frac{\partial}{\partial y_5}, \frac{\partial}{\partial \theta_1}, \cdots, \frac{\partial}{\partial \theta_5} \right\}^T \tag{5}$$

$$\nabla^{\dot{q}} = \left\{ \frac{\partial}{\partial \dot{x}_1}, \cdots, \frac{\partial}{\partial \dot{x}_5}, \frac{\partial}{\partial \dot{y}_1}, \cdots, \frac{\partial}{\partial \dot{y}_5}, \frac{\partial}{\partial \dot{\theta}_1}, \cdots, \frac{\partial}{\partial \dot{\theta}_5} \right\}^T \tag{6}$$

The movement equation of the mechanical system is, then, given by the *Generalized Hamilton's Principle*:

$$\frac{\mathrm{d}}{\mathrm{d}t} \left(\nabla^{\dot{q}} \otimes \mathcal{L} \right) - \nabla^q \otimes \mathcal{L} + \nabla^{\dot{q}} \otimes \mathcal{F} = \mathbf{Q}^{ext} \tag{7}$$

where $\otimes$ represents the *tensorial product*. This product together with the nabla operators represent the *gradient* of the function they are applied on.

2.1 Restrictions to the Movement

The current state of the modeling of the mechanical system does not describe precisely its behavior. It is necessary to impose to it some restrictions that will help to describe the existing Coulomb's friction between parts.

These restrictions are imposed to the system via the *Lagrange Multipliers Method*.

2.1.1 Coulomb's Friction Between Tank Bottom and Feet Plates

In order to evaluate the force required to keep the active part (1st rigid body in Fig. 1) in its position relative to the tank bottom (5th body), it is required to define that, being the relative angles of the two bodies positive or negative, the last contact point of one body to another shall not slide.

So, in terms of position, the constraint can be written as follows:

$$
\begin{aligned}
f_1(\mathbf{q}) \quad = \quad & \sec(\theta_1 - \theta_5)(x_1 \cos \theta_1 + (y_1 + H_b) \sin \theta_1 + L_{f_p}) + \\
& + \tan(\theta_1 - \theta_5)(x_5 \sin \theta_5 - y_5 \cos \theta_5) - (x_5 \cos \theta_5 + y_5 \sin \theta_5) = constant
\end{aligned} \tag{8}
$$

where:

- $p = 1$ if $\theta_1 \geq \theta_5$, and $p = N_f$ otherwise;

- H_b is the distance of the active part's center of gravity to the feet plates.

This constraint can be written in terms of the generalized velocities and accelerations:

$$\frac{\mathrm{d}f_1}{\mathrm{d}t} = (\nabla^q \otimes f_1) \cdot \dot{\mathbf{q}} = 0 \tag{9}$$

$$\frac{\mathrm{d}^2 f_1}{\mathrm{d}t^2} = \dot{\mathbf{q}} \cdot [(\nabla^q \otimes f_1 \otimes \nabla^q) \, \dot{\mathbf{q}}] + (\nabla^q \otimes f_1) \cdot \ddot{\mathbf{q}} = 0 \tag{10}$$

where:

- (¨) represents the second order time-derivative of a parameter of the mechanical system;

- $(\nabla^q \otimes f_1)$ is the gradient of the constraint in terms of the generalized coordinates;

- $(\nabla^q \otimes f_1 \otimes \nabla^q)$ is the Hessian matrix of the constraint in terms of the generalized coordinates.

The constraint is valid while the friction force required is lower than the limit force to slide (friction coefficient times normal force, μN).

2.1.2 Coulomb's Friction Between Core Limbs and Active Part

So far no connections were defined between the active part of the transformer and its most extreme core limbs.

That is because the connection is mainly defined by existing contact between the core steel sheets of these bodies in the superposed regions. These regions of sheet's superposition are also known as the *Step Lap* regions.
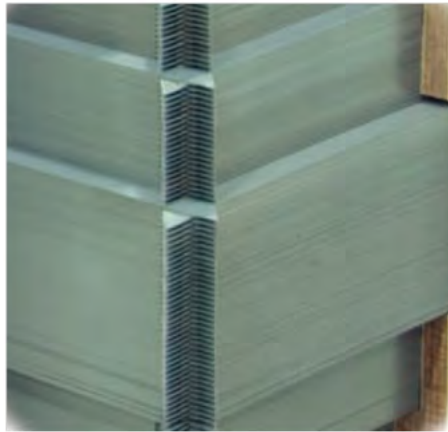
(a) Superposition of Core Steel Sheets – *Step Lap*

(b) Representation of the Step Lap

(c) Damaged Step Lap Region

Figure 2: Step Lap Region

As can be seen in Fig. 2a, the two groups of steel sheets are stacked alternately, which defines the superposed region. Once the sheets are pressed, the existing friction between them prevents relative displacement until the critical limit for sliding is reached.

In order to evaluate the limit values for sliding of a plane body it is necessary to compute the resultant forces and moments due to the friction (shear) stress in the superposed regions. Goyal (1989) presents a calculation methodology for evaluation of resultant forces and moment in a sliding planar body.

So, consider a plane body in imminent sliding. In this condition the friction stress acting punctually in the whole body has the following amplitude:

$$\|\boldsymbol{\tau}\| = \mu p \tag{11}$$

where μ is friction coefficient and p is the pressure applied on the body.

To determine the direction of the friction, consider the Fig. 3. The instantaneous movement of the plane body can be defined as a rotational movement around a center of rotation.

F. Torres and L. Driemeier
Integrity Assessment Of Power Transformer Under Dynamic Loads
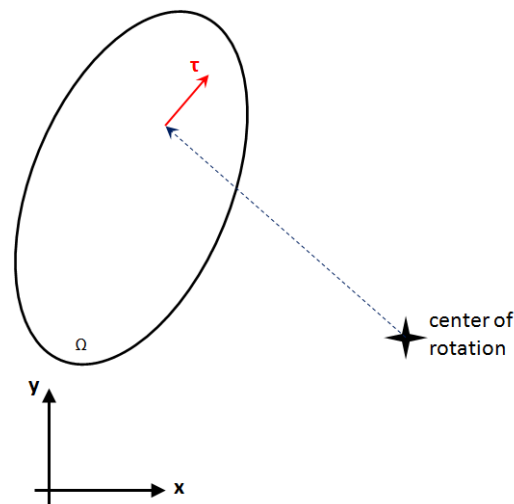
Figure 3: Friction Stress in a Plane Body

Then, for a center of rotation $\{x_c, y_c\}^T$, the direction of the friction stress in any point of the body can be defined as:

$$\hat{\boldsymbol{\tau}} = \frac{1}{\sqrt{(x-x_c)^2 + (y-y_c)^2}} \left\{ \begin{array}{c} y - y_c \\ x_c - x \end{array} \right\} \tag{12}$$

The resultant forces and moment (according to the origin of the coordinate system) are, then, defined as follows:

$$F_x(p, x_c, y_c) = \iint_\Omega \frac{\mu p (y - y_c)}{\sqrt{(x-x_c)^2 + (y-y_c)^2}} \mathrm{d}x \mathrm{d}y \tag{13}$$

$$F_y(p, x_c, y_c) = \iint_\Omega \frac{-\mu p (x - x_c)}{\sqrt{(x-x_c)^2 + (y-y_c)^2}} \mathrm{d}x \mathrm{d}y \tag{14}$$

$$M(p, x_c, y_c) = \iint_\Omega \frac{-\mu p [x(x - x_c) + y(y - y_c)]}{\sqrt{(x-x_c)^2 + (y-y_c)^2}} \mathrm{d}x \mathrm{d}y \tag{15}$$

where Ω is the area which the friction stress acts on.

The components of friction force and friction moment are, then, determined in a direct way by the value of pressure applied on the body and the coordinates of the center of rotation.

In order to evaluate the forces to keep the extreme limbs attached to the active part, it is necessary to impose restrictions to the system movement.

Consider L the horizontal distance between the centers of gravity of active part and frontal limb (for instance). Consider also $\{d_x, d_y\}^T$ as the accumulated slid distances of the limb.

Then, for the non-sliding condition, the following equality is valid:

$$\left\{ \begin{array}{c} L + x_2 \\ y_2 \end{array} \right\} = \left[\begin{array}{cc} \cos\theta_1 & -\sin\theta_1 \\ \sin\theta_1 & \cos\theta_1 \end{array} \right] \left\{ \begin{array}{c} L + d_x \\ d_y \end{array} \right\} + \left\{ \begin{array}{c} x_1 \\ y_1 \end{array} \right\} \tag{16}$$

Equation (16) imposes the restriction over the position of the bodies. In order to impose the restriction over the velocities and accelerations, each directional component of the Eq. (16) shall be time differentiated.

$$f_2(\mathbf{q}) = (L + d_x)\cos\theta_1 - d_y \sin\theta_1 + x_1 - L - x_2 = 0 \tag{17}$$

$$\frac{\mathrm{d}f_2}{\mathrm{d}t} = (\nabla^q \otimes f_2) \cdot \dot{\mathbf{q}} = 0 \tag{18}$$

$$\frac{\mathrm{d}^2 f_2}{\mathrm{d}t^2} = \dot{\mathbf{q}} \cdot [(\nabla^q \otimes f_2 \otimes \nabla^q)\dot{\mathbf{q}}] + (\nabla^q \otimes f_2) \cdot \ddot{\mathbf{q}} = 0 \tag{19}$$

$$f_3(\mathbf{q}) = (L + d_x)\sin\theta_1 + d_y\cos\theta_1 + y_1 - y_2 = 0 \tag{20}$$

$$\frac{\mathrm{d}f_3}{\mathrm{d}t} = (\nabla^q \otimes f_3) \cdot \dot{\mathbf{q}} = 0 \tag{21}$$

$$\frac{\mathrm{d}^2 f_3}{\mathrm{d}t^2} = \dot{\mathbf{q}} \cdot [(\nabla^q \otimes f_3 \otimes \nabla^q)\,\dot{\mathbf{q}}] + (\nabla^q \otimes f_3) \cdot \ddot{\mathbf{q}} = 0 \tag{22}$$

Equations (17) to (22) allows the evaluation of the components of the restriction force in horizontal and vertical directions. In order to determine the moment, the following restriction must be imposed:

$$f_4(\mathbf{q}) = \theta_1 - \theta_2 - \theta_{acc} = 0 \tag{23}$$

$$\frac{\mathrm{d}f_4}{\mathrm{d}t} = (\nabla^q \otimes f_4) \cdot \dot{\mathbf{q}} = 0 \tag{24}$$

$$\frac{\mathrm{d}^2 f_4}{\mathrm{d}t^2} = \dot{\mathbf{q}} \cdot [(\nabla^q \otimes f_4 \otimes \nabla^q)\,\dot{\mathbf{q}}] + (\nabla^q \otimes f_4) \cdot \ddot{\mathbf{q}} = 0 \tag{25}$$

where θ_{acc} is the accumulated difference (slid) of angles between active part and frontal limb and f_i are the restriction equations in terms of position (*Holonomic Restrictions*).

The imposed restrictions to the movement of the limbs give the forces and moment necessary to keep them solidary to the active part. With these values, it is possible solve the inverse problem and find the pressure and center of rotation coordinates of Eq. (13) to (15). When the required pressure is greater than the existing one specified in the design, the sliding occurs.

3. IMPLEMENTATION

The system of differential equations of the mechanical system is solved explicitly via *Runge-Kutta 4th order* method. In order to establish the scheme of implementation, consider the *state vector*, $\mathbf{v}$:

$$\mathbf{v} = \left\{ \begin{array}{c} \mathbf{q} \\ \dot{\mathbf{q}} \end{array} \right\} \tag{26}$$

Equation (7) can be rewritten in the following manner:

$$\mathbf{M}\ddot{\mathbf{q}} = -(\nabla^{\dot{q}} \otimes \mathcal{F}) - (\nabla^q \otimes U) + \mathbf{Q}^{ext} \tag{27}$$

where:

- $\mathbf{M}$ is the diagonal mass matrix of the system;
- $\mathbf{Q}^{ext}$ is vector of generalized external loads;
- $(\nabla^q \otimes U)$ is the gradient of the potential energy in terms of the generalized coordinates;
- $(\nabla^{\dot{q}} \otimes \mathcal{F})$ is the gradient of the *Rayleighian* in terms of the generalized velocities.

Writing the dynamic equations in *State Space Representation* yields:

$$\begin{bmatrix} \mathbf{I} & \mathbf{0} \\ \mathbf{0} & \mathbf{M} \end{bmatrix} \left\{ \begin{array}{c} \dot{\mathbf{q}} \\ \ddot{\mathbf{q}} \end{array} \right\} = \begin{bmatrix} \mathbf{0} & \mathbf{I} \\ \mathbf{0} & \mathbf{0} \end{bmatrix} \left\{ \begin{array}{c} \mathbf{q} \\ \dot{\mathbf{q}} \end{array} \right\} + \left\{ \begin{array}{c} \mathbf{0} \\ \mathbf{Q}^{ext} - (\nabla^q \otimes U) - (\nabla^{\dot{q}} \otimes \mathcal{F}) \end{array} \right\}$$

$$\mathbf{A}\dot{\mathbf{v}} = \begin{bmatrix} \mathbf{0} & \mathbf{I} \\ \mathbf{0} & \mathbf{0} \end{bmatrix} \mathbf{v} + \left\{ \begin{array}{c} \mathbf{0} \\ \mathbf{Q}^{ext} - (\nabla^q \otimes U) - (\nabla^{\dot{q}} \otimes \mathcal{F}) \end{array} \right\} \tag{28}$$

Equations (9), (10), (18), (19), (21), (22), (24) and (25), which represent the restrictions in terms of velocity and acceleration, can be rewritten as:

$$\mathbf{J}(\mathbf{v})\dot{\mathbf{v}} + \mathbf{b}(\mathbf{v}) = \mathbf{0} \tag{29}$$

where $\mathbf{J}(\mathbf{v})$ represents the gradient of the restrictions $((\nabla^q \otimes f_i))$ and $\mathbf{b}(\mathbf{v})$ represents the quadratic forms in terms of the generalized velocities as consequence of the second order time-derivative the holonomic restrictions $(\dot{\mathbf{q}} \cdot [(\nabla^q \otimes f_i \otimes \nabla^q) \, \dot{\mathbf{q}}])$.

As exposed by Lanczos (1949), the restriction forces are normal to the restriction itself. For the mechanical system here described, all external forces are applied by means of restrictions. Therefore:

$$\mathbf{Q}^{ext} = \mathbf{F}^{restr} = \mathbf{J}^T \boldsymbol{\lambda} \tag{30}$$

Assembling the restriction equations with the state space representation of the system yields:

$$\begin{bmatrix} \mathbf{A} & -\mathbf{J}^T \\ -\mathbf{J} & \mathbf{0} \end{bmatrix} \left\{ \begin{array}{c} \dot{\mathbf{v}} \\ \boldsymbol{\lambda} \end{array} \right\} = \begin{bmatrix} \mathbf{0} & \mathbf{I} \\ \mathbf{0} & \mathbf{0} \\ \mathbf{0} & \mathbf{0} \end{bmatrix} \mathbf{v} + \left\{ \begin{array}{c} \mathbf{0} \\ -(\nabla^q \otimes U) - (\nabla^{\dot{q}} \otimes \mathcal{F}) \\ \mathbf{b}(\mathbf{v}) \end{array} \right\}$$

$$\mathbf{A}^{xt} \left\{ \begin{array}{c} \dot{\mathbf{v}} \\ \boldsymbol{\lambda} \end{array} \right\} = \mathbf{B}\mathbf{v} + \left\{ \begin{array}{c} \mathbf{0} \\ -(\nabla^q \otimes U) - (\nabla^{\dot{q}} \otimes \mathcal{F}) \\ \mathbf{b}(\mathbf{v}) \end{array} \right\} \tag{31}$$

where $\boldsymbol{\lambda}$ are the *Lagrange Multipliers*

At every evaluation of the slide conditions, the determination of the Step Lap region is necessary to be performed. As can be seen in Fig. 2b and 2c, the region of the Step Lap which the friction stress acts on can be determined by the intersection of two polygons. Weiler and Atherton (1977) present a methodology to determine the resultant polygon from the intersection of two others. Such algorithm was implemented to evaluate the superposed regions of the magnetic core.

4. RESULTS

For the following design parameters, a comparison between results of two different compressive loads of the active part is shown.

- Active Part Mass (without extreme limbs): 47 t;
- Extreme Limb Mass (each): 9 t;
- Tank Mass: 50 t;
- Vehicle Mass: 4.6 t;
- Tank Height: 3970 mm;

- Tank Length: 3620 mm;
- Initial Velocity: 1.1 km/h;
- Peak Deceleration: 0.6 g (5886 mm/s^2);
- Deceleration Time: 0.1 s.

These are typical values for power transformers.
The deceleration function of the vehicle is presented in Fig. 4.
Two situations were evaluated:

1. The active part is installed inside the tank with no interference against the tank cover;

2. The active part is installed inside the tank with its wooden blocks in interference against tank cover, such that it is initially pressed with 10 t against bottom.

In these situations, the results for friction in tank bottom and reactions in top and bottom arresting devices are compared
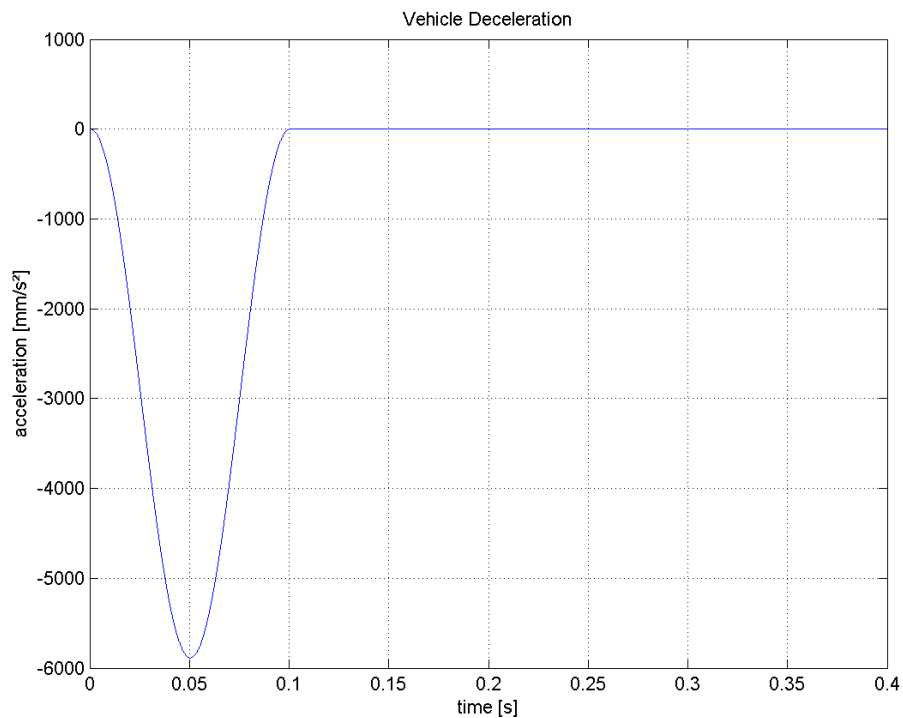
Figure 4: Deceleration of Vehicle

4.1 Active Part and Vehicle's Angles
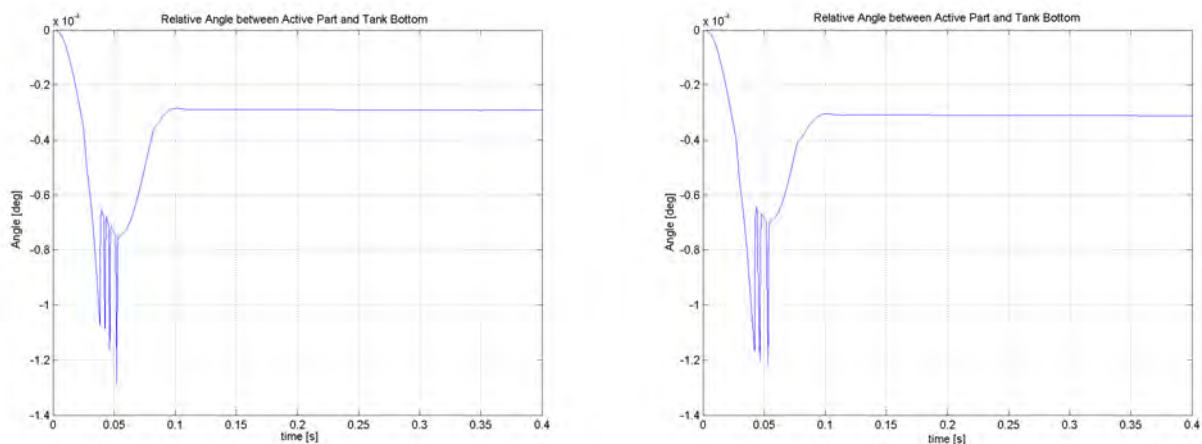
(a) Condition of No Interference   (b) Condition of Interference

Figure 5: Active Part and Vehicle's Angles

It is possible to notice that, in both situations, close to moment when the load is the most intense, the relative angle presents an oscillation. This fact can be explained by the stick-slip behavior of the friction force during this period.

Also, it can be seen that, in both conditions, the active part presents a negative angle relative to the tank bottom after the load, although with less intensity for condition *with interference*.

4.2 Tank Bottom's Friction

Figure 6 presents the results of friction force of the contact of the active part with the tank bottom. It is possible to notice that, in both conditions, the friction force presents oscillation in two different moments.

As can be seen confirmed in Fig. 7, the first oscillation presented occurs during a moment when the active part is sliding on the tank bottom. This oscillation, then, can interpreted as an *stick-slip* movement.
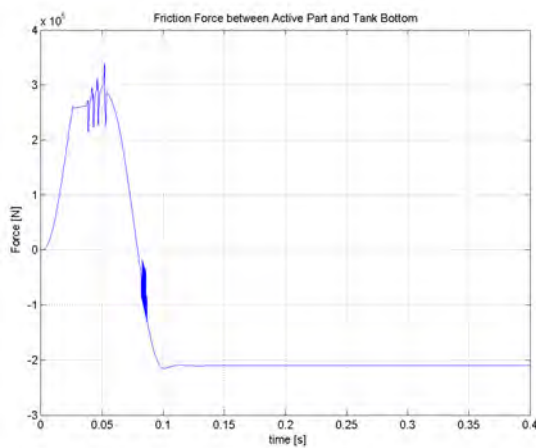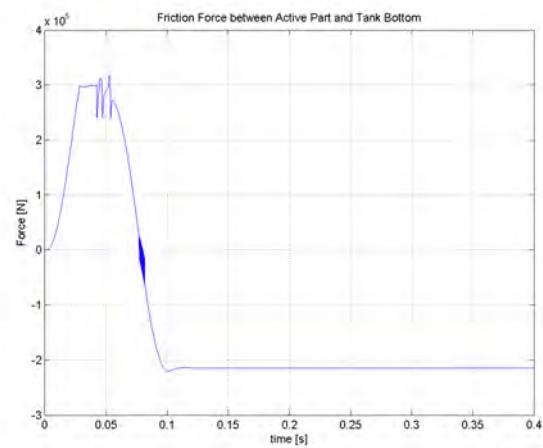
(a) Condition of No Interference (b) Condition of Interference

Figure 6: Friction Force of Active Part on Tank Bottom
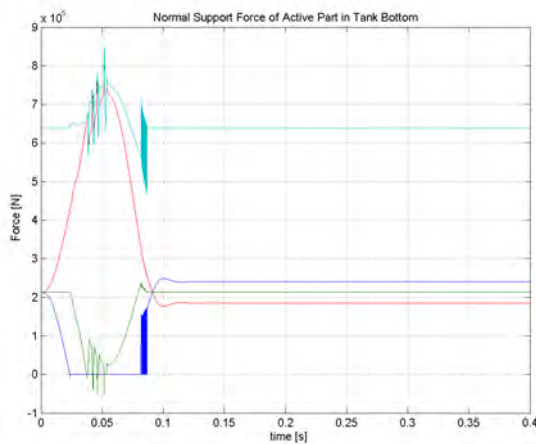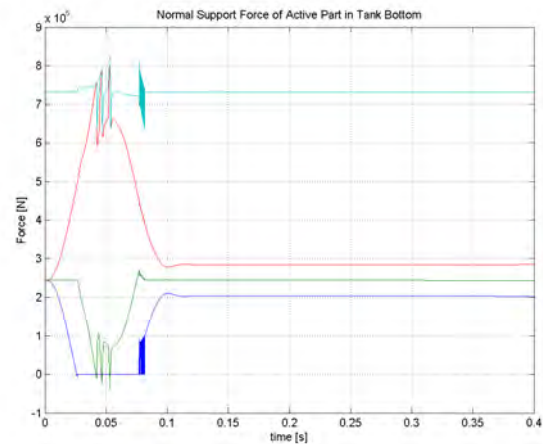
(a) Condition of No Interference (b) Condition of Interference

Figure 7: Normal Force on Feet Plates

The second oscillation occurs when the contact of one of the feet plates with the tank bottom is again reestablished. However, in this condition, once the active part was not presenting relative movement, the *stick-slip* phenomenon was not observed.

4.3 Arresting Devices' Reactions

It is possible to notice that in all the conditions, during the beginning of the deceleration of the vehicle, none of the arresting devices are really effective, playing their role only after a certain slide starts taking place.

Comparing both situations, the condition *with interference against tank cover* the reaction forces on the bottom arresting devices were slightly higher than in the *no interference* condition. This was because, once the normal forces on tank bottom are higher in the condition *with interference*, the friction force that impedes the active part of returning to its original position are, consequently higher, being balanced by the bottom arresting devices.

5. CONCLUSIONS

It was possible to notice that slight changes in design parameters may have a significant influence on the dynamic response of the equipment.

Such differences in dynamic response are not easily understood by the current design practices adopted in market.

By evaluating quantitatively the dynamic response of transformers being transported, it is possible to distinguish how and which parameters have to be focused in order to strengthen the equipment's behavior and make it more reliable to withstand any sort of mechanical load during its transportation.
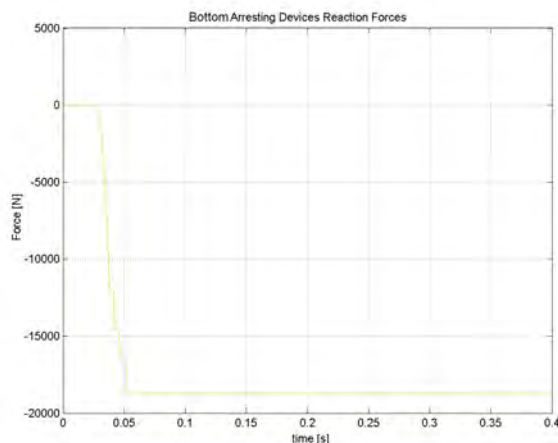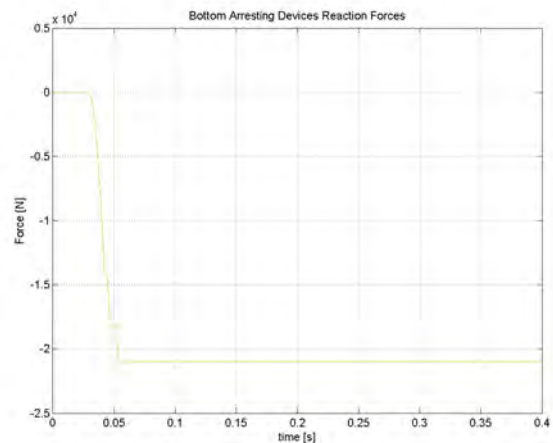
(a) Condition of No Interference   (b) Condition of Interference

Figure 8: Reaction Forces on Bottom Arresting Devices
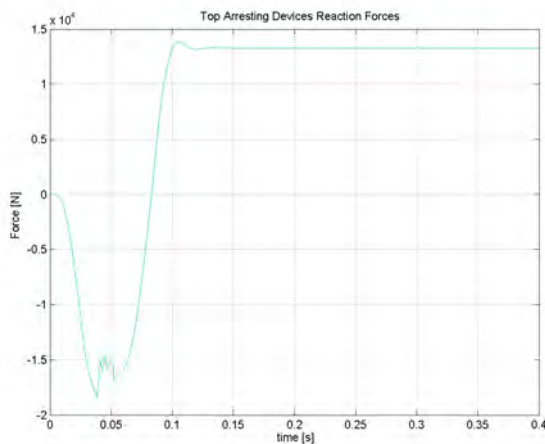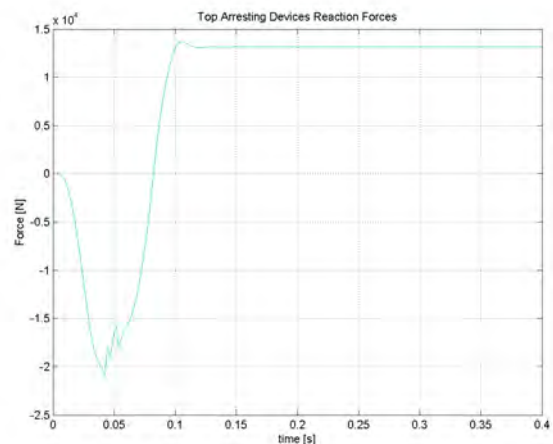
(a) Condition of No Interference   (b) Condition of Interference

Figure 9: Reaction Forces on Top Arresting Devices

6. REFERENCES

Dick, E.P. and Erven, C.C., 1978. "Transformer diagnostic testing by frequency response analysis". *Power Apparatus and Systems, IEEE Transactions on*, Vol. PAS-97, No. 6, pp. 2144 –2153. ISSN 0018-9510. doi: 10.1109/TPAS.1978.354718.

Goyal, S., 1989. *Planar Sliding of a Rigid Body with Dry Friction: Limit Surfaces and Dynamics of Motion*. Ph.D. thesis, Cornell University, Ithaca, NY, USA.

Lanczos, C., 1949. *The Variational Principles of Mechanics*. University of Toronto Press, Toronto, 1st edition.

Pleite, J., Gonzalez, C., Vazquez, J. and Lazaro, A., 2006. "Power transformer core fault diagnosis using frequency response analysis". In *Electrotechnical Conference, 2006. MELECON 2006. IEEE Mediterranean*. pp. 1126 –1129. doi:10.1109/MELCON.2006.1653298.

Pleite, J., Olias, E., Barrado, A., Lazaro, A. and Vazquez, J., 2002. "Transformer modeling for fra techniques". In *Transmission and Distribution Conference and Exhibition 2002: Asia Pacific. IEEE/PES*. Vol. 1, pp. 317 – 321 vol.1. doi:10.1109/TDC.2002.1178342.

Secue, J.R. and Mombello, E., 2008. "Sweep frequency response analysis (sfra) for the assessment of winding displacements and deformation in power transformers". *Electric Power Systems Research*, Vol. 78, No. 6, pp. 1119 – 1128. ISSN 0378-7796. doi:10.1016/j.epsr.2007.08.005. URL http://www.sciencedirect.com/science/article/pii/S037877960700171X.

Sim, H.J., Digby, S.H. and Harlow, J.H., 2004. "Equipment types: Power transformers". In *Electric Power Transformer Engineering*, CRC Press LLC, Boca Raton, USA, chapter 2, pp. 23–44. 1st edition.

Weiler, K. and Atherton, P., 1977. "Hidden surface removal using polygon area sorting". In *Proceedings of the 4th*

F. Torres and L. Driemeier
Integrity Assessment Of Power Transformer Under Dynamic Loads

annual conference on Computer graphics and interactive techniques. ACM, New York, NY, USA, SIGGRAPH '77, pp. 214–222. doi:10.1145/563858.563896. URL `http://doi.acm.org/10.1145/563858.563896`.

7. RESPONSIBILITY NOTICE

The authors are the only responsible for the printed material included in this paper.